

# Effect of curing history on ultimate glass transition temperature and network structure of crosslinking polymers

Shu-Sing Chang

Polymers Division, Materials Science and Engineering Laboratory, National Institute of Standards and Technology, Gaithersburg, MD 20899, USA

(Received 31 July 1991; accepted 8 February 1992)

For a particular crosslinking polymer, it is often considered that the final state of crosslinking may be reached by post-curing at temperatures above its ultimate glass transition temperature,  $T_{g,u}$ , regardless of previous curing histories. Although this appears to be true over a certain range of variation in curing history, the  $T_{g,u}$  and the network structure depend strongly on the curing history over a wide range of conditions for the homopolymerization of diglycidyl ether of bisphenol-A (DGEBA) catalysed by 2-ethyl-4-methyl imidazole. As degrees of cure and crosslink increase, the glass transition temperature,  $T_g$ , of a sample may increase from the monomeric DGEBA value of  $-22^\circ\text{C}$  to the highest value near  $180^\circ\text{C}$ . Depending on the curing thermal history, some samples may only attain a  $T_{g,u}$  of  $\sim 100^\circ\text{C}$ , even after post-curing at  $200^\circ\text{C}$  for 16 h. Although the influence of thermal history on  $T_g$  may rank second after the influence of the degree of cure, it is the most important factor on  $T_{g,u}$  for a fixed resin and catalyst composition. The reversible physical ageing process appears to be the least influential on  $T_g$ . As all crosslinking reactions involve competing reactions with different kinetic parameters, we believe that these phenomena are universally observable to a greater or lesser degree in all crosslinking reactions.

(Keywords: crosslinking network; cure monitoring; differential scanning calorimetry; diglycidyl ether of bisphenol-A; 2-ethyl-4-methyl imidazole; glass transition temperature; thermal analysis; thermal history; thermoset resins)

## INTRODUCTION

Diglycidyl ether of bisphenol-A, DGEBA, is a popular base epoxy resin. It is often cured with amines, anhydrides or phenols, with or without the use of catalysts or accelerators such as 2-ethyl-4-methyl imidazole, EMI. In these applications, the high temperature etherification is considered as a side reaction. By using a catalytic amount of EMI in the order of 2–4%, DGEBA homopolymerizes through etherification into a product which is highly stable to at least  $200^\circ\text{C}$  with a glass transition temperature,  $T_g$ , of  $\sim 160^\circ\text{C}$ . It is also highly chemical-resistant due to the ether linkages, and possesses good electrical properties. Unlike the widely used linear homopolymer polyethylene, the crosslinked homopolymer based on this popular epoxy monomer DGEBA has not been well studied<sup>1–10</sup>. The purpose of this work is to establish the relationship between curing histories and the properties of the final product. The findings of this work on the effects of thermal history should be generally observable in other network-forming systems.

The  $T_g$  of monodispersed linear polymers increases as the degree of polymerization increases. At high degrees of polymerization, the  $T_g$  levels off at a maximum value  $T_{g,\infty}$ . For a large number of polymers, the simple expression<sup>11</sup>:

$$T_{g,\infty} - T_{g,M} = k/M \quad (1)$$

may be used to describe the  $T_g$  as a function of the molecular weight,  $M$ , provided that the  $M$  is higher than low oligomers. For instance, the  $T_g$  of monodispersed

atactic polystyrene at an  $M$  of  $> 5000$  can be well represented<sup>12</sup> by equation (1) with the constants  $T_{g,\infty} = 378\text{ K}$  and  $k = 10^5$ . Thus, the  $T_g$  of polystyrene remains relatively unchanged to within 1 K at  $M$  of  $> 100\,000$ .

A similar form of equation (1) was given<sup>13,14</sup> for the trend of  $T_g$  of crosslinked polymers as a function of the molecular weight between the crosslinks,  $M_c$ :

$$T_{g,M_c} - T_{g,0} = k_c/M_c \quad (2)$$

where  $T_{g,0}$  is the glass transition temperature of the uncrosslinked infinite molecular weight polymer of the same composition and  $k_c$  is  $\sim 4 \times 10^4$  as an average for several cases<sup>15</sup>. Thus, the  $T_g$  of a crosslinked polymer is increased from the  $T_g$  of the base linear polymer as the  $M_c$  is reduced. A more involved form was given by DiMarzio<sup>16</sup> for crosslinked rubber:

$$(T_g - T_{g,0})/T_{g,0} = k_1 X_c / (1 - k_2 X_c) \quad (3)$$

where  $X_c$  is the crosslinking density and is inversely related to  $M_c$ . A widely quoted equation as attributed to DiBenedetto assumes a similar form, which was given a basis on the principle of corresponding states<sup>17</sup>. By considering the backbone  $T_{g,0}$  is not equal to  $T_{g,\infty}$  and changes as a function of molecular weight as in equation (1), Stutz *et al.*<sup>18</sup> modified the DiBenedetto equation to include the effect of both crosslinking density and the increase of the  $T_g$  of the uncrosslinked polymer backbone as the degree of cure increases.

As this paper was being reviewed, a paper was published<sup>19</sup> which gave a comprehensive overview on the

subject of  $T_g$  as a function of conversion in thermosetting polymers and a theory for the  $T_g$  of a polyfunctional novolac epoxy crosslinked with a novolac resin, which showed a rather steep increase in  $T_g$  at the last stage of cure.

Regardless of how the maximum crosslinking density or the minimum average  $M_c$  may be calculated from the maximum degree of cure, the theoretical maximum  $T_g$  for a crosslinked polymer may not be realized because the reaction generally stops at a certain high degree of cure, e.g.  $\sim 90$ – $95\%$ , due mainly to topographic constraints. Furthermore the structure of the actual crosslinked polymer is highly complex. Not only are there different  $M_c$  values but there are also different terminations of the crosslinking branches, and the variations in the concentrations of end groups and trapped monomers and oligomers. One must also deal with various types of molecular entities between the crosslinks and how to represent their contributions to various properties with a single parameter such as  $M_c$  or  $X_c$ .

Polymerization of linear polymers is generally designed to terminate at a particular molecular weight. For crosslinking reactions, the reaction does not stop until almost all reactants are used up. The reaction may virtually cease when the material develops into a glassy state at the curing temperature. However, the reaction involving the remaining reactants resumes when the material is heated above the  $T_g$ . In practice, there appears to exist an ultimate glass transition temperature,  $T_{g,u}$ , for each resin. A common belief is that by post-curing the resin in the rubbery state at temperatures above the  $T_{g,u}$ , the resin would reach a maximum degree of cure regardless of its previous curing history. However, the following observations will show that, although a stable resin is produced by post-curing at high temperatures, the resultant  $T_{g,u}$  can be strongly influenced by the history during cure. Curing in several isothermal stages, such as by gelation at different low temperatures, may change the  $T_{g,u}$  by  $\sim 10$  K. By quickly bringing the raw resin mixture to temperatures in its eventual rubbery state, the attainable  $T_{g,u}$  may be reduced by some 50 K. There is however a window within which the  $T_{g,u}$  appears to be relatively insensitive to curing histories.

Physical ageing without causing any further chemical reaction may change the  $T_g$  or the fictive temperature of the glass transition slightly<sup>20</sup> by  $\sim 10$  K. The physical ageing phenomena are however reversible, as heating to temperatures in the rubbery state will eliminate the previous history of glass formation.

The intention of this work is to show that a single parameter, such as the degree of cure,  $M_c$  or  $X_c$ , may only be used to approximately characterize a crosslinked polymer under 'normal curing conditions'. It is however far from a complete description of the cured material. In order to save time and energy, and to increase productivity, industrial processes are pushed towards the fastest reaction conditions possible. It is in this regime of fast heating rates that more drastic changes in the  $T_{g,u}$  and the structure of the final network occur.

The phenomena shown as an example here should be universally observable in other crosslinking systems. However the changes in the  $T_{g,u}$  may be less pronounced in reactions of high activation energies. In these cases, for any realistic sample sizes, the low thermal conductivity of the polymeric material is not sufficient to allow the removal of the heat generated by the exothermic

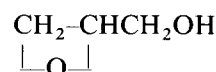
reaction to maintain a near isothermal condition. Therefore the near-adiabatic temperature rise causes a self-accelerating runaway reaction to occur. The runaway reaction produces final products that are relatively similar to each other due to the similarity in their curing thermal histories.

## EXPERIMENTAL

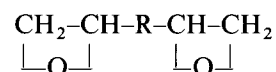
### Materials

Three commercially available low molecular weight DGEBA resins were used (Dow Chemical DER332, Shell Chemical EPON825 and EPON828)\*. Resins containing higher monomer contents crystallize more readily. The first two products contain 97–99% of the monomeric DGEBA and tend to crystallize at room temperatures around 22°C. The resin EPON828 may crystallize to a lesser degree after standing for a long time at room temperature. Purified DGEBA monomer crystals were prepared from the above commercial resins by recrystallizing from a mixture of 4-methyl-2-pentanol and 4-methyl-2-pentanone<sup>21</sup>, or from the solvent-rich phase of methanol or ethanol solutions<sup>6</sup>. Purified DGEBA monomer melts at 41.4°C with a heat of fusion of 81 J g<sup>-1</sup>. Molten DGEBA monomer can easily be cooled to a glass. The  $T_g$  of DGEBA monomer is  $-22^\circ\text{C}$  with a heat capacity discontinuity<sup>6</sup>,  $\Delta C_p$ , of  $\sim 0.60$  J g<sup>-1</sup> K<sup>-1</sup>.

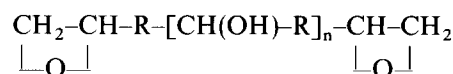
DGEBA may be considered as the condensation product of glycidol:



and bisphenol-A,  $\text{C}(\text{CH}_3)_2(p\text{-C}_6\text{H}_4\text{OH})_2$ . The basic hydrocarbon building block in bisphenol-A,  $\text{C}(\text{CH}_3)_2(p\text{-C}_6\text{H}_4\text{-})_2$ , is relatively stiff and may be represented by  $\text{-B-}$ . The group between the epoxy groups may be represented by  $\text{-R-}$ , which is composed of  $\text{-CH}_2\text{-O-B-O-CH}_2\text{-}$ . Thus, the DGEBA monomer may be represented as:



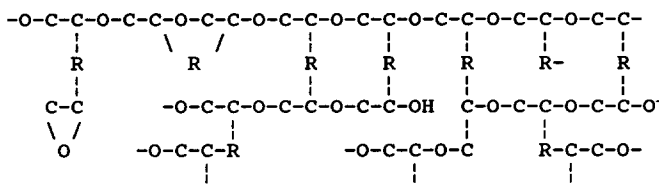
and the DGEBA oligomers as:



The homopolymerization of DGEBA occurs through a nucleophilic attack on the epoxy ring, followed by the propagation of the  $\text{-O}^-$  ion or hydroxyl group to form ethers. When fully branched, the glycidyl group assumes a basic configuration of  $\text{-O-CH}_2\text{-CH}(\text{CH}_2\text{-O-})\text{O-}$ . The homopolymer may be viewed as having polyether chains of poly(oxyethylene) crosslinked by the group  $\text{-R-}$ . The skeleton of the network may be represented as follows to show a variety of crosslinking and termination configurations, with some of the epoxy rings opened to

\* Certain commercial materials and equipment are identified in this paper in order to specify adequately the experimental procedure. In no case does such identification imply recommendation or endorsement by the National Institute of Standards and Technology, nor does it imply necessarily the best available for the purpose.

form active  $-O^-$  ions or hydroxyl groups:



The crosslinks of the cured resin are further complicated by the presence of a few per cent of DGEBA-EMI adducts. A small amount of unreacted DGEBA monomer and oligomers may also be present or trapped.

The catalyst, 2-ethyl-4(5)-methyl imidazole, EMI, of 99% purity was used without further purification. Solid EMI melts in the range of 40–45°C and stays in the liquid state for a long time at room temperature.

The values of  $T_g$  are high<sup>6,8</sup> in the range of ~150–180°C for an EMI concentration of 2–4 parts per hundred parts resin by weight (phr, Figure 1). A fixed composition of 3 phr EMI in DGEBA was used throughout this paper to minimize the effect of varying catalyst concentration.

Differential scanning calorimetry

A commercial differential scanning calorimeter (Perkin-Elmer DSC-7) and its associated Perkin-Elmer 7500 series computer was used. Although the instrument's minimum digitizing resolution for differential power is ~0.3 μW, the typical noise level varies in the order of 2–10 μW peak-to-peak with a period of 0.1–2 min, depending on operational conditions. The reproducibility in the middle of a long scan is however often observed in the order of 50–100 μW, which also happens to be the range of isothermal drift observed in a period of ~1 h. These figures may be used to estimate the uncertainties for integration within a scan and in heat capacity and heat of reaction calculations involving multiple scans.

In order to minimize the effect of baseline drifts during the scan and their influence on the interpretation of the data, most of the thermal analysis data were reduced to a representation of the heat capacity of the sample. This type of representation provides the ease of comparison, although a negative value of heat capacity has no meaning in the equilibrium sense, but it is used to show

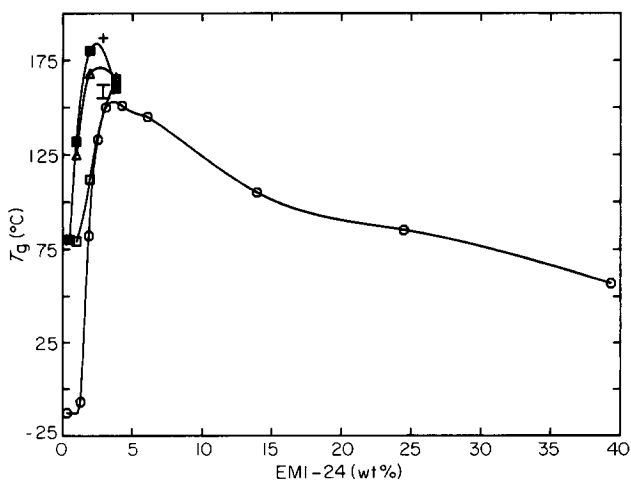


Figure 1 Glass transition temperature as a function of EMI content. Reference 6: (Δ)  $T_{iso}=80^\circ\text{C}$  then scan post-cured; (□) scanned at  $10\text{ K min}^{-1}$ ; (■) scanned at  $1\text{ K min}^{-1}$ . Reference 8: (○)  $T_g$  onset. This work: (+) maximum  $T_{g,u}$  observed; (I) scanned at  $10\text{ K min}^{-1}$

the occurrence of an exothermic event. When the thermogram of a d.s.c. scan indicated an apparent  $C_p$  other than that expected of a normal vibrational heat capacity contribution, either an exothermic or endothermic phenomenon is superimposed on the heat capacity curve.

All scanning runs require the observation of steady isothermal periods at both initial and final temperatures of a scan. A blank run may be subtracted from the sample runs to minimize the effect of mismatch in the instrument. No heating rate corrections were applied to the time-temperature transformation. The apparent shift in the melting point of indium was observed at  $\sim 0.075\text{ K}/(\text{K min}^{-1})$  due to thermal lags in the system. Low thermal conductivities of polymeric samples would cause further thermal lags in reaching a steady state. The temperature non-uniformity in the sample holder of  $< 1\text{ K}$  is relatively small<sup>22</sup> in comparison to that in a low thermal conductivity organic or polymeric sample at high heating rates or high exothermic heat releases<sup>23</sup>.

Heat of reaction

The maximum degree of cure and the maximum heat of cure,  $Q_{max}$ , is commonly obtained in d.s.c. studies by integrating the exothermic peak area of a heat flow curve, as the sample is scanned to a certain maximum temperature just before any noticeable degradation takes place. The degree of cure,  $\alpha$ , of a partially cured or isothermally cured sample which is lower than the maximum cure, is commonly estimated by the heat released from the remaining fraction of the reactant during a post-cure scan,  $Q_{pc}$ , to the maximum temperature, thus:

$$\alpha = (Q_{max} - Q_{pc}) / Q_{max} \quad (4)$$

In an ideal case, the integrated peak area  $Q$  may yield the enthalpy difference between the product p and the reactant r at the final temperature  $T_f$  (Figure 2):

$$Q \approx \Delta H_{T_f} = (H_p - H_r)_{T_f} \quad (5)$$

with the assumption that the liquidus heat capacity of the product is close to and follows a smooth extension of the liquidus heat capacity of the reactant<sup>24</sup>, and that

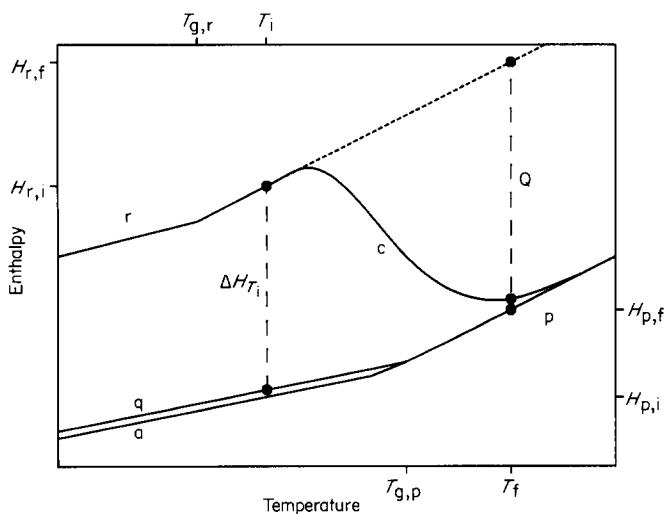


Figure 2 Schematic representation of enthalpy changes for the curing reaction and physical ageing: (r) raw resin reactant; (p) polymerized resin product; (c) curing path; (q) quenched glass; (a) annealed glass; (i) initial scan temperature; (f) final scan temperature; (Q) heat from peak integration

there are no contributions from the reaction at the limits for integration.

However, in practice, the peak integration of a single curing curve may contain a number of sources of uncertainties. The choice of integration limits is somewhat subjective. The commonly used linear baseline between the integration limits may not represent the liquidus heat capacities of the reactant and the product. Also, contributions from heat releases at the limits may have been neglected.

Therefore, instead of depending only on a single curing curve and an assumed baseline to obtain a heat of cure,  $Q$ , the heat of reaction at the initial scan temperature,  $\Delta H_{T_i}$ , may be obtained through a well-defined thermodynamic cycle, by involving a subsequent scan on the cured resin over the same temperature limits<sup>6</sup>. Assuming that the degree of cure does not change between the end of the curing scan and the beginning of the second scan,  $\Delta H_{T_i}$  is simply the difference between the integrals of the two scan curves in their entirety, from the initial temperature  $T_i$  to the final temperature  $T_f$ , including any thermal effects occurring isothermally at  $T_f$  (Figure 2):

$$\Delta H_{T_i} = (H_{p,T_f} - H_{r,T_i}) - (H_{p,T_f} - H_{p,T_i}) = (H_p - H_r)_{T_i} \quad (6)$$

This procedure reduces the uncertainties due to the arbitrariness in assigning integration limits on a single curing curve.

The second scan is generally needed to indicate the  $T_g$  of the resin just cured. In both scans, isothermal observations at the beginning and at the end of a scan are required as the integration limits and to minimize the effect of baseline drifts from the background heat flow. The isothermal period at the high temperature end of the curing scan may be extended until the heat effects from curing fall within the noise level. Conversion of these curves into a heat capacity type of representation by subtracting contributions from sample containers and holders is desirable for comparison purposes, but not essential in the heat of reaction calculation.

The heat of reaction at other temperatures, especially between the  $T_g$  of the monomer and that of the polymer, may be calculated by adjusting for the differences in the heat capacities of the reactant and the product. The heat capacities of the monomer and the resultant polymer in their solidus states, whether in the crystalline state or in the glassy state, are close to each other. Likewise, the liquidus heat capacities of the monomer and the resultant polymer above their respective  $T_g$ s are also similar. Therefore, the heats of reaction at temperatures below the  $T_g$  of the monomer or above the  $T_g$  of the polymer remain relatively constant.

Enthalpy differences from post-curing scans may also be obtained in a similar procedure involving two scans.

#### Glass transition temperature

The  $T_g$  of a crosslinked system is generally somewhat ill-defined. Not only is there a distribution of molecular weights or segmental lengths between the crosslinking points, but there are also distributions of unreacted functional groups and monomers which happen to be trapped or fixed in spatial arrangements throughout the network. Therefore the macroscopic glass transition phenomena occur over a relatively wide temperature region, e.g.  $\sim 50$  K. Slow cooling at a constant rate may be used to sharpen the glass transition observation by introducing a relaxation peak at a few degrees above the

fictional temperature. Although annealing at a temperature below the  $T_g$  can also produce a relaxation peak, relaxation peaks may be produced throughout the wide  $T_g$  region. Examples of such occurrences have been reported for crosslinked polymers<sup>25</sup> and for homogeneous bimodal mixtures of linear polymers<sup>26</sup>.

We defined the  $T_g$  used here as the temperature at which the enthalpy line of a glassy state intersects with that of the supercooled liquid or rubbery state upon heating. This definition depends only on the conditions under which a glass was formed during cooling and is independent of the heating rate at which the glass transition is observed. Therefore it applies to all observations with or without the appearance of a relaxation peak for an annealed glass or the occurrence of an exotherm for a quenched glass. In the case of slow-cooled or annealed glass, where relaxation peaks are observed above the  $T_g$ , this intersecting temperature is often called the fictive temperature. For fast-cooled glasses, e.g. cooled at  $\sim 50$ – $100$  K  $\text{min}^{-1}$  through the glass transition region, the intersecting temperature occurs near the maximum rate of heat capacity increase or near the mid-point of the heat capacity rise from the glassy state to the supercooled liquid or rubbery state.

For the present system, the glass transition region ends quite sharply at the rubbery region,  $T_1$ , which occurs at  $\sim 10$  K above the assigned  $T_g$ . The onset of the glass transition region from the glassy state occurs rather gently and is ill-defined. Because of the imprecision in the determination of the heat capacity over a wide scan temperature range and the failure to separate spontaneous relaxations from vibrational contributions by means of thermal analytical methods, the uncertainty to assign an onset of the  $T_g$  is fairly large. A positive second derivative of heat capacity with respect to temperature is generally not expected from Debye or Einstein functions at moderate temperatures. Heat capacities of polymers at moderate temperatures generally have a long region of linear temperature dependence<sup>27,28</sup>. This is expected if the vibrational spectrum has a relatively even distribution in the region of  $100$ – $1000$   $\text{cm}^{-1}$ , e.g. there exists one frequency in each of the  $100$   $\text{cm}^{-1}$  segments<sup>29</sup>.

## RESULTS

There were over 300 d.s.c. runs performed on various batches of DGEBA mixtures with 3 phr EMI. It is not possible to discuss the details of individual runs here. Only summaries and generalized observations are given below.

#### Scan cure

Scan curing is a preferred method to yield the heat of reaction to the maximum extent. In the isothermal method, the extent of reaction is incomplete as the reaction stops when the resin reaches a glassy state.

The scan curing schedule consisted of the following: (1) heating to an initial temperature, e.g.  $50^\circ\text{C}$ , (2) after waiting for a temperature equilibrium, observation of the background heat flow for a short time, e.g. 1 min, (3) a scan at a desired heating rate to  $200$  or  $250^\circ\text{C}$ , and (4) a 2–10 min observation of the background heat flow at the  $T_f$ . After the sample was cooled to  $50^\circ\text{C}$  at the maximum rate of the instrument, the cured sample was re-scanned with the same schedule as above for the characterization of the  $T_g$  of the cured sample. In order to develop the ultimate glass transition temperature,  $T_{g,u}$ ,

**Table 1** Scan cure of DGEBA with 3 phr EMI<sup>a</sup>

Sample series no.	dT/dt (K min <sup>-1</sup> )	T <sub>pre</sub> (°C)	T <sub>max</sub> (°C)	T <sub>post</sub> (°C)	-dQ/dt <sub>max</sub> (W g <sup>-1</sup> )	-Q <sub>c</sub> (J g <sup>-1</sup> )	-Q <sub>pc</sub> (J g <sup>-1</sup> )	-ΔH <sub>rxn,50</sub> (J g <sup>-1</sup> )	T <sub>g</sub> (T <sub>1</sub> ) <sub>10</sub> (°C)	T <sub>g</sub> (T <sub>1</sub> ) <sub>s</sub> (°C)	ΔC <sub>p</sub> (J g <sup>-1</sup> K <sup>-1</sup> )
1	0.1		60		0.07	450			172 (185)		0.20
11	0.1	57	64		0.07	500			184 (186)		0.13
12	0.1		66		0.08	410			158 (174)		0.18
13	0.1		60		0.05	340			183 (196)		0.20
11	1	81	89	101	0.28	484			187 (193)		0.04
1	2		96	134	0.23	243	4		175 (186)		0.17
9	2		104		1.06	464		433	170 (185)	168 (185)	0.20
1	5		107		1.7	417	15		165 (185)		0.16
9	5		116		2.0	467		425	168 (178)	161 (181)	0.14
3	10		130		4.8	410			157 (175)		0.25
9	10		124	138	3.0	426		440	159 (170)		
10	10		125	142	2.8	450		442	162 (173)		0.21
12	10		125	145	2.4			426	155 (170)		0.20
13	10	118	124	149	1.4		21	390	150 (165)		0.15
13	10	113	121	149	1.3		7	485	143 (156)		0.25
1	20		137	154	4.7	325+	50		140 (148)		0.26
2	20		137	150	4.2	288+	100		150 (160)		0.19
3	20		139	150	5.3	322+	40		150 (158)		0.19
9	20		138	155	5.6	379+		440	143 (152)		0.26
9	40		149	175	6.3	300+	60	440	132 (145)	129 (136)	0.26
13	50	144	150	190	3.1		5	365	135 (155)	85 (94)	0.30
12	60		154	194	7.2			410	119 (127)	102 (118)	0.34
11	100		160	>200	4.8		280	400	144 (155)	100 (105)	0.20
12	100		169	(205)	10			355	106 (116)	91 (103)	0.37
12	100		168	(204)	9.8			355	106 (116)		0.29
13	150		171	>200	5.4		6	350	136 (147)		0.30
10	200		180	>200	12		353		133 (140)		
11	200		177	>200	5.1		350	410	150 (158)	122 (137)	0.21
12	200		189	(220)	12.5			340	99 (109)	95 (103)	0.35
12	200		187	>200	14			365	125 (134)		0.28

<sup>a</sup> dT/dt, rate of curing; T<sub>pre</sub>, temperature at pre-main peak; T<sub>max</sub>, temperature at main peak; T<sub>post</sub>, temperature at post-main peak; dQ/dt<sub>max</sub>, maximum rate of heat release at main peak; Q<sub>c</sub>, integrated heat releases from all three peaks; Q<sub>pc</sub>, integrated heat releases from post-curing scan; ΔH<sub>rxn,50</sub>, heat of reaction at initial scan temperature of 50°C; T<sub>g</sub> and T<sub>l</sub>, glass transition temperature and liquidus temperature (observed at a scan rate of 10 K min<sup>-1</sup> or at the same rate as that of curing scan); ΔC<sub>p</sub>, heat capacity rise from the glass to supercooled liquid at T<sub>g</sub>. Samples are made of commercial grade DGEBA, except series 11 and 13 which are made of recrystallized DGEBA

the cured sample may be subjected to a further soaking at 200°C for 2–24 h, and then re-scanned. The T<sub>g</sub> hardly changed > 5°C, if the resin had been scanned to 250°C or after 1–2 h at 200°C. The DGEBA with 3 phr EMI resin system is highly stable at 200°C. No appreciable weight losses were detected in most runs. Only a few runs indicated a weight loss in the order of 0.2%. Some degree of degradation may occur at temperatures above 220–230°C. T<sub>g</sub> may be lowered slightly after standing at 250°C for a long period. The results of curing scans at different scan rates and post-cured scans are summarized in Table 1.

D.s.c. scans during the cure of samples from series 9 are shown in Figure 3 as typical thermograms in a heat capacity type of representation. The maximum rate of heat release during cure may be estimated from the

apparent C<sub>p</sub> value at the peak of the exotherm multiplied by the heating rate. Additional heat release, especially at high heating rates, during the isothermal period at the final scan temperature is not shown. The enthalpy changes from the enthalpy of the reactant at 50°C, occurring during the cure, are shown in Figure 4. It is obvious that by assigning the heat of reaction as the enthalpy difference between two temperatures chosen arbitrarily on the curing curve, the heat release, Q, may be subject to large uncertainties. The heat of reaction should be defined at a reaction temperature as described earlier by a two-scan procedure.

During the scan cure, besides the major exothermic peak (main peak), there were two other exothermic peaks or shoulders observable. At low heating rates, a rather small peak or shoulder before the main peak (pre-main

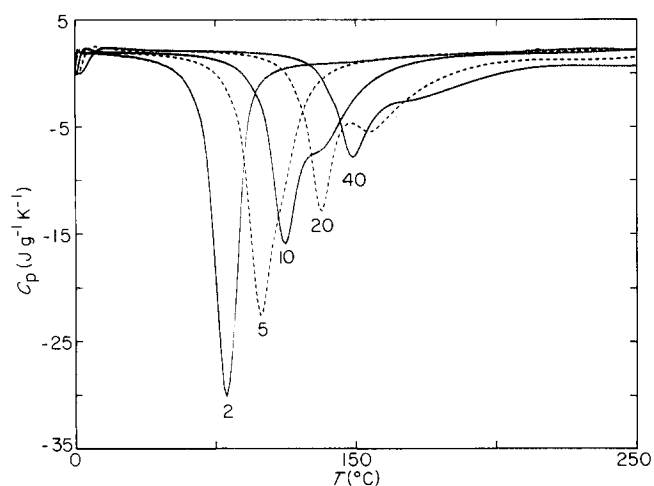


**Figure 3** Scan curing of DGEBA with 3 phr EMI. The numbers shown denote the heating rate (in  $\text{K min}^{-1}$ )

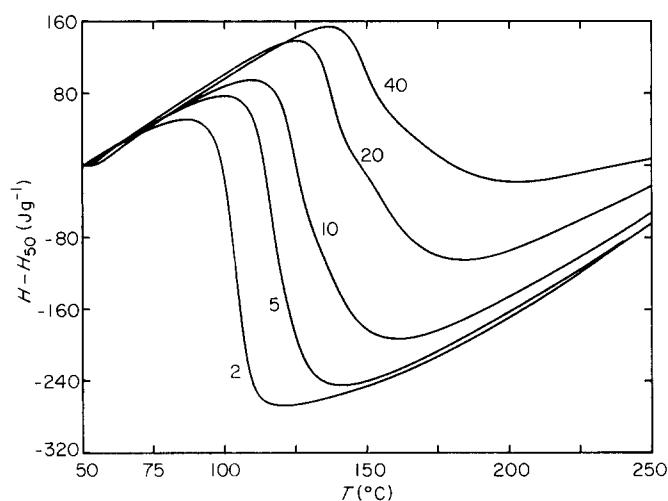


**Figure 4** Enthalpy change during scan cure of DGEBA with 3 phr EMI. The numbers shown denote the heating rate (in  $\text{K min}^{-1}$ )

peak) was barely resolved by enlarging the initial portions of the curve. The pre-main peak is considered to be due to the initiation of adduct formation between EMI and DGEBA. At high heating rates, another hump appeared after the main peak (post-main peak). This post-main peak is considered due to  $-\text{OH}$  propagation, while the main peak is considered to be due to oxonium ion propagation. The peak temperatures appeared to follow an exponential law with the heating rate, *Figure 5*, as a consequence of reaction kinetics and thermal lag in the instrument. Both pre- and post-main peaks were more pronounced with highly purified DGEBA monomer. At high rates of scan, the energy involved in the post-main peak can be greater than that of the main peak. It appears that the diminishing of the intensity of the main peak, by not allowing enough time for the main reaction to reach completion, may be the major cause for the lowering of the ultimate  $T_g$ . During the curing scan, the resident time is generally not sufficient for the reaction to proceed to the maximum extent. Therefore the thermogram at the end of the scan may contain contributions from the reaction besides the contributions from the heat capacity (aside from the instrumental background heat flow). Integration of the curve alone without adding the contribution from a slow reaction at

the end will generally yield a smaller value for the heat of reaction.

The second scan following the cure generally showed only a relatively smooth curve with the occurrence of a glass transition. A small amount of further heat releases in the order of  $10 \text{ J g}^{-1}$  were seen only for samples cured at very high curing rates, e.g.  $100\text{--}200 \text{ K min}^{-1}$ . Samples cured at scan rates of  $< 2 \text{ K min}^{-1}$  and then fast-cooled produced resins with an inconspicuous glass transition of small  $\Delta C_p$  through the glass transition region. In order to enhance the detection of the glass transition of these samples, these samples required slow cooling, e.g. at  $0.1 \text{ K min}^{-1}$ , or annealing at temperatures below the  $T_g$ . Such physically aged samples generally give rise to a relaxation peak or a sharper glass transition on heating.

#### *Isothermal cure*

Thermosetting resins are generally cured in a single or multiple-step quasi-isothermal mode in the composite manufacturing process. The temperature of a raw resin mixture or a B-staged resin is raised to the curing temperature and held there until the reaction subsides. Most studies on curing kinetics and cure development are observed isothermally in the early stage of cure, until the resin develops into a glassy state. A post-cure schedule at higher temperatures may be applied for the reaction to reach a maximum degree of conversion (near 95%).

In the d.s.c. isothermal curing experiment, the raw resin mixture was heated to the isothermal curing temperature,  $T_{\text{iso}}$ , at a heating rate of  $200 \text{ K min}^{-1}$  and then held at  $T_{\text{iso}}$  until the rate of heat releases from cure subsides close to the background heat flow. Typical isothermal thermograms are shown in *Figure 6*, where the abscissa scales are in minutes and the numbers shown denote  $T_{\text{iso}}$ . The isothermally cured resin was then fast-cooled to  $50^\circ\text{C}$  and post-cured by scanning from  $50$  to  $200$  or  $250^\circ\text{C}$  at a rate of  $10 \text{ K min}^{-1}$ . If the sample was isothermally cured below  $150^\circ\text{C}$ , heat releases from the post-curing scan were observed at temperatures just above the  $T_g$  which occurred at  $10\text{--}20 \text{ K}$  above  $T_{\text{iso}}$ . If a post-cure exotherm was observed, the sample was

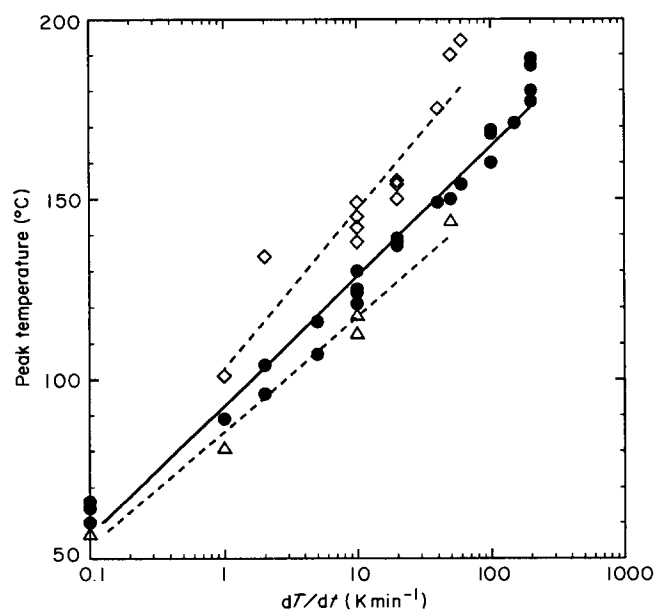


**Figure 5** Peak temperature as a function of scan rate: (●) main peak; (△) pre-main peak; (◇) post-main peak

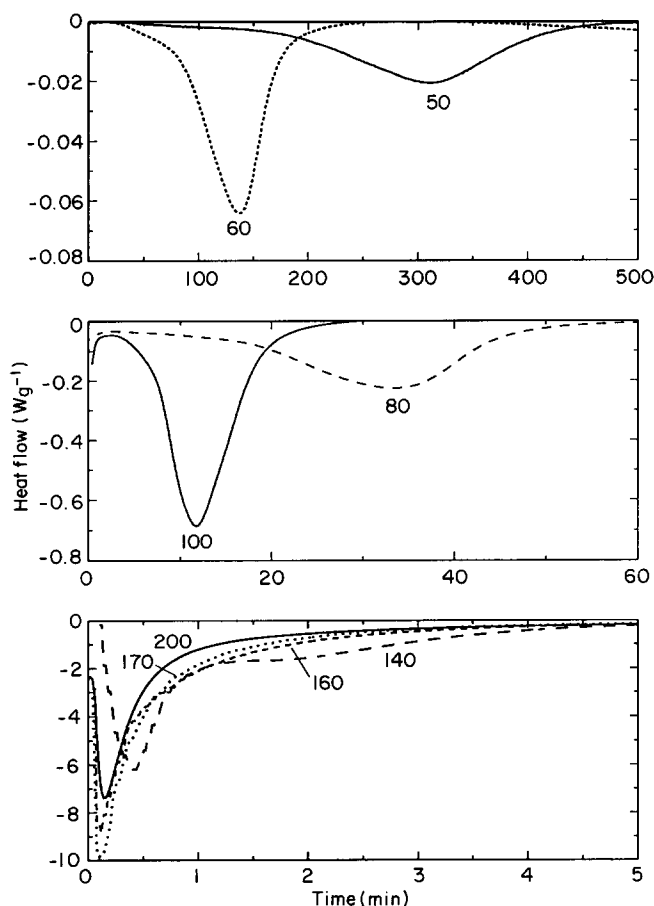


Figure 6 Exotherms during isothermal cure. The numbers shown denote isothermal curing temperatures (in °C)

scanned a second time for the  $T_g$  of the post-cured sample. If the sample had only been exposed to 200–250°C for 2–5 min, soaking at 200°C was used for the development of  $T_{g,u}$ . It appeared that after soaking for 2 h at 200°C,  $T_g$  reached an asymptote and did not change >1–2 K even after a soaking time of up to 20 h. Slight degradation was suspected from the d.s.c. thermogram at temperatures of >220–230°C. However no weight losses >0.2%, due to volatiles, were detected.

By enlarging the initial portion of the isothermal curve, a small exothermic peak or shoulder (pre-main peak) was observed to precede the main peak at curing temperatures below 100°C. This peak appeared at about one-third of the time for the main peak. The peak height of the pre-main peak was only about one-tenth of that of the main peak. Heise and Martin<sup>8</sup> also observed a small peak at 8 min with the main peak occurring at 22 min for the curing of a mixture of 100 mol DGEBA with 5 mol EMI at 80°C. The pre-main peak is considered to be due to the initiation of adduct formation between EMI and DGEBA. At high isothermal curing temperatures, e.g. from 100 to 140°C, there was an additional peak (post-main peak) after the main peak. The peak height of the post-main peak was about one-third of that of the main peak and occurring at around two to four times the main peak time. This post-main peak is considered due to –OH propagation, while the main peak is considered to be due to oxonium ion propagation. The magnitudes of both the pre- and post-main peak appeared more pronounced with purified DGEBA of higher monomeric content. The small pre-main peak dis-

appeared if the resin mixture was left at room temperature for several hours or overnight. Ageing at room temperature would cause the main peak to diminish and to shift to higher temperatures. Figure 7 shows the relationship between the peak times and isothermal curing temperature.

The integration of the isothermal curve is rather imprecise, especially at lower curing temperatures where the curing time is long and the background is noisy. The determination of zero heat production is difficult. Therefore the integrated value tends to be smaller than the actual value. The same error applies to the integration of scan runs with long isothermal observation at the  $T_f$ . The time at which the rate of the reaction exotherm is diminished to the noise level of the instrument is considered to be the time when the reaction appeared to have ceased. At high isothermal temperature, even during a short period of time to bring the resin mixture from room temperature to the isothermal temperature at a rate of 200 K min<sup>-1</sup>, some reaction may already have occurred. The amount of exotherm during the scan at 200 K min<sup>-1</sup> was estimated to be 40 J g<sup>-1</sup> to 170°C and 120 J g<sup>-1</sup> to 200°C. This may be estimated from a scan at 200 K min<sup>-1</sup>. On the other hand, although the slow heat releases of a sample left at room temperature for 1 week (10 000 min) was not measurable by d.s.c., it appears to be equivalent to a curing of 350 min at 50°C. Therefore the integration of isothermal curves suffers from baseline noise at low temperatures and incomplete integration at high temperatures.

As stated earlier, isothermally cured samples require additional post-curing to fully develop the cure. The first scan post-cure is used to indicate the  $T_g$  and the degree of cure of the sample as isothermally cured. The heat of reaction obtained as the sum of isothermal heat releases and the heat of post-cure is not as reliable as the heat of reaction measured by scan curing. A subsequent scan is used to characterize the fully cured sample. The results

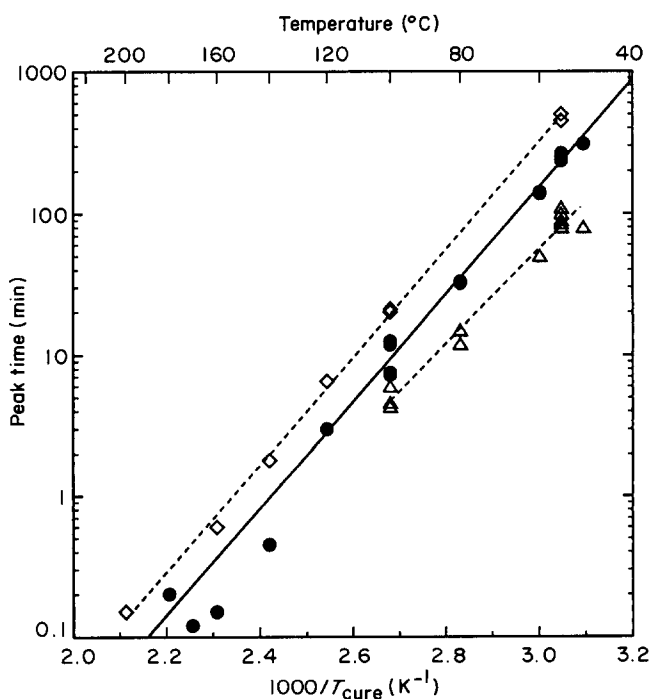


Figure 7 Peak time as a function of isothermal cure temperature: (●) main peak; (△) pre-main peak; (◇) post-main peak

**Table 2** Isothermal cure of DGEBA with 3 phr EMI<sup>a</sup>

Sample series no.	$T_{\text{iso}}$ (°C)	$t_{\text{pre}}$ (min)	$t_{\text{max}}$ (min)	$t_{\text{post}}$ (min)	$-dQ/dt_{\text{max}}$ (W g <sup>-1</sup> )	$-Q_{\text{iso}}$ (J g <sup>-1</sup> )	$-Q_{\text{pc}}$ (J g <sup>-1</sup> )	$T_{\text{g,iso}}$ (°C)	$T_{\text{g}}(T_1)$ (°C)	$\Delta C_p$ (J g <sup>-1</sup> K <sup>-1</sup> )
2	50	80	310		0.021	205		(75)	168 (193)	0.15
2	50						93	(83)	162 (187)	0.16
3	55	85	255	(450)	0.021	210	125	78	(185)	
3	55	100	242		0.029	170	120	78	171 (178)	
4	55		260		0.031	197	132	60	174 (183)	
6	55	110	265		0.023	140	107	77	182 (198)	
6	55	90	236		0.028	308	93	67	183 (195)	
7	55	80	242	(500)	0.030	272	109	75		
1	60	50	138		0.065	255			167 (182)	0.13
2	60		141		0.066	257	> 100	82	164 (184)	0.19
1	80	(15)	32		0.30	286	> 70	(92)	172 (185)	0.30
2	80						67	(95)	151 (163)	0.19
2	80								166 (177)	0.16
10	80	(12)	33		0.23	330	97	(95)	166 (182)	0.17
5	100		11.8		0.69	357	45	(100)	168 (182)	0.08
5	100	(6)	12.5		0.63	306	72	(110)	168 (178)	0.25
8	100	4.6	7.5	20	0.47	290	90	(110)	174 (186)	0.15
8	100	4.3	7.2	21	0.45	288	93	(110)	183 (200)	
5	120		3.0	6.5	1.7	415	50	(135)	158 (177)	0.18
10	140		0.45	1.8	6.2	477	16	(155)	165 (176)	0.14
10	160		0.15	(0.6)	8.9	446			158 (170)	0.18
13	160				> 2.5	440			172 (187)	0.13
10	170		0.12		9.9	430		132	150 (161)	0.22
13	180		0.2		4.9	440			143 (160)	0.24
10	200			0.15	7.4	353		131	138 (143)	0.25
12	200		(0.2)		6.6	350/411		122	150 (158)	0.21

<sup>a</sup>  $T_{\text{iso}}$ , isothermal cure temperature;  $t_{\text{pre}}$ , time at pre-main peak;  $t_{\text{max}}$ , time at main peak;  $t_{\text{post}}$ , time at post-main peak;  $dQ/dt_{\text{max}}$ , maximum rate of heat releases at main peak;  $Q_{\text{iso}}$ , heat releases at  $T_{\text{iso}}$ ;  $Q_{\text{pc}}$ , heat releases from post-curing scan;  $T_{\text{g,iso}}$ , glass transition temperature after isothermal cure;  $T_{\text{g}}$  and  $T_1$ , glass transition temperature and liquidus temperature observed at 10 K min<sup>-1</sup> after post-curing;  $\Delta C_p$ , heat capacity rise at  $T_{\text{g}}$ . Samples are made of commercial grade DGEBA, except series 7, 8 and 13 which are made of recrystallized DGEBA

of isothermal cure and subsequent post-cure are given in Table 2.

## DISCUSSION

### Reaction mechanism

The basic scheme of the reaction mechanism for the catalytic homopolymerization of DGEBA has been proposed by Farkas and Strohm<sup>1</sup>, that the imine and the epoxy forms a 1:1 hydroxyl adduct which forms a 1:2 alkoxide ion adduct with a second epoxy as the effective catalyst. The 1:1 adduct of EMI and phenyl glycidyl ether (PGE) was also found to be an excellent curing catalyst<sup>1</sup>. The resins studied were cured at 50°C for 24 h and then post-cured at 140°C for 24 h. Approximately 70% of the epoxy groups were reacted after 50°C, and ~92% after 140°C. Other studies<sup>2,3,5,30-33</sup> have suggested refinements to the proposed mechanism. Ricciardi *et al.*<sup>31,32</sup> suggested that imidazole is regenerated during the cure; this was supported by another study<sup>5</sup>. Most of these studies concentrated on reactions

between different types of imidazole and PGE<sup>2,3,30</sup>, cresyl glycidyl ether<sup>33</sup> or other monoepoxies to elucidate the mechanism of different stages of the homopolymerization, rather than the reaction of DGEBA with EMI as the catalyst. 2-Methylimidazole was also found to be an effective catalyst<sup>1</sup> as well as dimethylbenzylamine<sup>1</sup>. Monosubstituted 1-methylimidazole was also effective<sup>3</sup>.

Berger and Lohse<sup>33</sup> showed that isopropanol accelerates the reaction. Jones *et al.*<sup>30</sup> showed an induction period for some reactions and the effect of the presence of other hydroxyl compounds, indicating the attack of epoxies also takes place via the hydroxyl group. Heise and Martin<sup>9</sup> also showed induction periods for the reaction, but considered the OH propagation to occur only at an EMI concentration of <5% and at high temperatures<sup>8</sup>.

A recent series of papers by Heise *et al.*<sup>7-10</sup> on the reaction of DGEBA and EMI agreed with the basic mechanism that at the initial stage there was adduct formation. The initial hump, corresponding to the pre-main peaks observed here, of ~5% heat release is



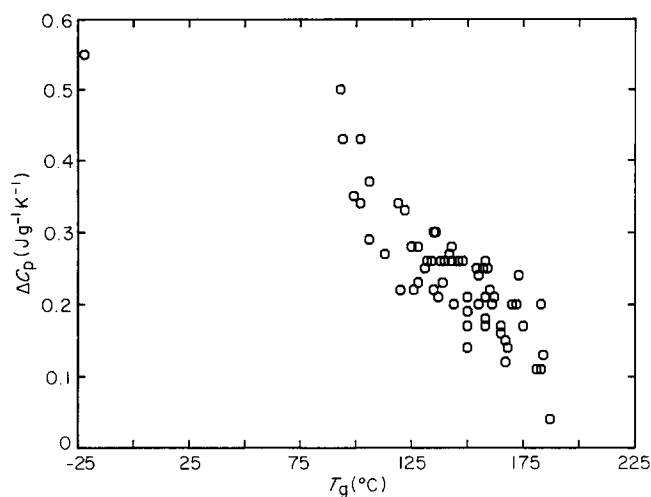


Figure 8 Heat capacity difference as a function of glass transition temperature

observed to be associated with the disappearance of the N–H band with little or no significant increase in  $T_g$ . The oxonium ion propagation is considered to be the principal reaction, with –OH propagation as a secondary reaction, corresponding to the post-main peaks observed here, occurring at higher temperatures and later times.

#### Heat of reaction

Barton<sup>34</sup> has corrected their earlier results for the PGE–EMI adduct to  $460 \text{ J g}^{-1}$ . The reported values of  $331 \text{ kJ g}^{-1}$  for 10:1 PGE–EMI<sup>5</sup> is probably in error as well as the description of the instrument and scanning to  $360^\circ\text{C}$ . Our earlier investigation<sup>6</sup> indicated a heat of reaction at  $50^\circ\text{C}$ ,  $\Delta H_{\text{rxn},50}$ , of  $425 \text{ J g}^{-1}$  for the 1:1 adduct and  $410 \text{ J g}^{-1}$  for the 1:2 adduct. The  $T_g$  of the 1:1 adduct is quite stable at  $95^\circ\text{C}$ , while that of the 1:2 adduct may decrease from  $77^\circ\text{C}$  upon heating to temperatures above  $150^\circ\text{C}$  due to degradation.

The value<sup>3</sup> for the heat of polymerization of  $410 \text{ J g}^{-1}$  (EMI content not specified) may also need correction as described earlier<sup>34</sup>. This correction would raise the value to  $530 \text{ J g}^{-1}$ . Our earlier studies<sup>6</sup> yielded a  $\Delta H_{\text{rxn},50}$  of  $540 \text{ J g}^{-1}$  for 2–4 phr EMI. Heise and Martin<sup>9</sup> gave a constant heat output of  $500\text{--}520 \text{ J g}^{-1}$  of DGEBA for a 4–40% EMI mixture. The maximum  $\Delta H_{\text{rxn},50}$  observed in this work is  $\sim 490 \text{ J g}^{-1}$ . A large number of scan cures from 2 to  $40 \text{ K min}^{-1}$  indicated a  $\Delta H_{\text{rxn},50}$  of  $440 \text{ J g}^{-1}$ . The sum of isothermal releases plus the heat of reaction in post-cure yield a lower value of around  $400 \text{ J g}^{-1}$  for  $T_{\text{iso}}$  above  $100^\circ\text{C}$ .

#### Heat capacity

The  $C_p$  of well cured DGEBA glass is quite linear from  $-50$  to  $100^\circ\text{C}$ . The temperature coefficient of the glassy  $C_p$  is slightly greater than that of the liquid. The liquidus or the rubbery heat capacity remained relatively constant at around  $2 \pm 0.2 \text{ J g}^{-1} \text{ K}^{-1}$ . As  $T_g$  is increased from  $-22^\circ\text{C}$ ,  $\Delta C_p$  is decreased from  $0.6 \text{ J g}^{-1} \text{ K}^{-1}$  at low temperatures to around  $0.1 \text{ J g}^{-1} \text{ K}^{-1}$  at  $\sim 180^\circ\text{C}$  (Figure 8). The diminishing of  $\Delta C_p$  to  $< 5\%$  of the  $C_p$  at the high end renders the high temperature  $T_g$  more difficult to detect.

It is generally observed that the heat capacities of the rubbery state or the supercooled liquid above the  $T_g$  are similar to each other regardless of the degree of cure. A

similar example exists for the liquidus heat capacity of a large variety of hydrocarbon polymers over a wide range of temperatures from 200 to 600 K. The liquid hydrocarbon heat capacity may be represented by a simple expression<sup>28</sup>:

$$C_{p,l} = 0.8 + 0.004T \quad (7)$$

to within 5%, where  $C_p$  is in  $\text{J g}^{-1} \text{ K}^{-1}$  and  $T$  is in K. A further generalization is that the heat capacity of the crosslinked polymer in the high temperature rubbery state is observed to be an extension of the low temperature liquidus heat capacity of the monomer<sup>24</sup>.

The  $C_p$  of a solid in the glassy state is lower than the liquidus  $C_p$  as described, and is within a few per cent of that in the crystalline state. For a partially cured sample, the  $C_p$  below  $T_g$  lies between that of a fully cured sample in its glassy state and that expected for a liquid.

For the present systems, the temperature coefficient of the heat capacity,  $dC_p/dT$ , for the glass below the  $T_g$  is higher than that for the supercooled liquid above the  $T_g$ . As the crosslinking density increases, the  $T_g$  increases with a diminishing  $\Delta C_p$ . It is then possible to view the temperature at which the  $C_p$  of the glass approaches that of the liquid as near the theoretical  $T_{g,u}$  of a system. Since temperature coefficients for the  $C_p$  of the glass and that of the liquid differ, therefore the assignment of the  $\Delta C_p$  is sensitive to both the extrapolation of the  $C_p$  values as well as the assignment of the  $T_g$ . The uncertainty of assigning the  $T_g$  is smaller in the case where  $dC_p/dT$  of the liquid is less than that of the glass.

#### Glass transition and ultimate glass transition temperature

The  $T_g$  may also be seen as a function of the EMI content as shown in Figure 1. The results of Heise and Martin<sup>8</sup> show that at low EMI content there is little  $T_g$  increase, presumably due mostly to linear chain propagation. The intermediate concentration of 3–5% EMI yielded the highest  $T_g$  as the result of high crosslinking density. As EMI concentration is increased further, more DGEBA will be consumed by DGEBA–EMI adduct formations and less DGEBA will be available for etherification. Hence  $T_g$  is lowered again. Although no details were given, it was also stated that, at  $< 5 \text{ mol EMI per } 100 \text{ mol epoxide}$ , a higher  $\Delta H$  and a higher  $T_g$  resulted from a slower heating rate and longer cure time.

Typical d.s.c. thermograms near the glass transition region for samples scan-cured at different heating rates are shown in Figure 9. The broken lines indicate the second scans which were heated at the same heating rate as the curing rate. Subsequent scans were heated at  $10 \text{ K min}^{-1}$  in order to offer a better comparison with other experiments. The differences between the two scan rates were rather small. No significant change or improvement in the  $T_{g,u}$  was observed by subsequent scans or post-curing. The resultant  $T_{g,u}$  appears to drop quite significantly as the scan rate was increased to around  $50 \text{ K min}^{-1}$ , as shown in Figure 10. The levelling off of  $T_{g,u}$  at higher heating rates may partially be due to the artifacts in d.s.c. measurement, as the indicated sample temperature lags behind the temperature of the instrument due to low thermal conductivity of the material.

After holding the sample for a reasonably long time at curing temperatures  $T_{\text{iso}}$  below  $150^\circ\text{C}$ , the developing of  $T_g$  virtually stopped at  $\sim 10\text{--}20 \text{ K}$  above  $T_{\text{iso}}$  (represented by the broken line in Figure 11). The sample left

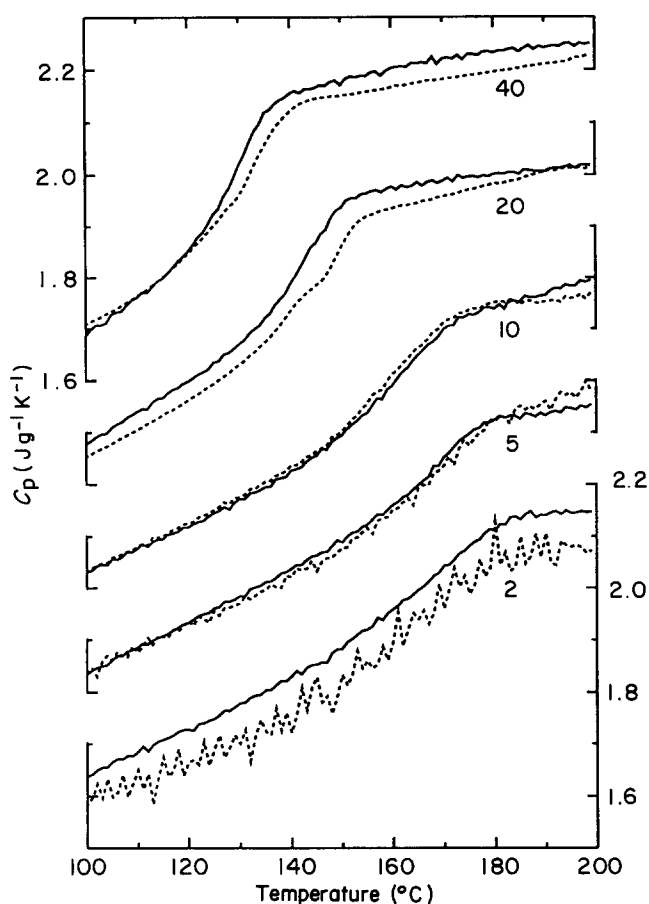


**Figure 9** Glass transition regions of scan cured DGEBA with 3 phr EMI. The numbers shown denote the heating rate during cure (in  $\text{K min}^{-1}$ ): (---) scanned at the same rate as scan cure; (—) scanned at  $10 \text{ K min}^{-1}$

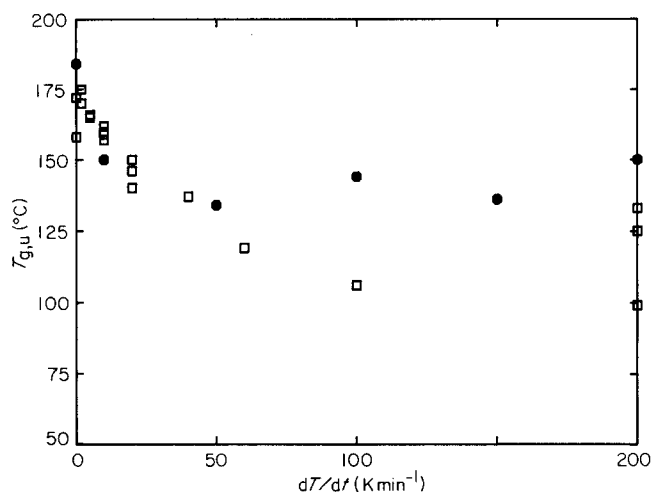


**Figure 10** Ultimate glass transition temperature as a function of curing rate: (□) commercial DGEBA resins with 3 phr EMI; (●) recrystallized DGEBA monomer with 3 phr EMI

at room temperature for 7 months showed a  $T_g$  of  $> 40 \text{ K}$  above the room temperature of  $\sim 22^\circ\text{C}$ . This is not only the result of prolonged soaking, but is also due to the higher molecular mobility in the less densely crosslinked glass formed at lower temperatures. The  $T_{g,u}$  after post-curing procedures for these samples was in the range of  $160\text{--}180^\circ\text{C}$ , depending on the initial  $T_{iso}$  and the raw resin constitution. Samples made from purified DGEBA monomer showed a slightly higher  $T_{g,u}$ . As often observed

in many systems, but seldom reported in any detail, samples left for a long time to gel at room temperature or below showed a slightly lower  $T_{g,u}$ . The  $T_{g,u}$  appeared to have reached a maximum at  $T_{iso}$  of  $\sim 100^\circ\text{C}$ . At a curing temperature of  $160^\circ\text{C}$ , the samples reached the  $T_{g,u}$  without further post-curing.

At  $T_{iso}$  of  $> 160^\circ\text{C}$ , the  $T_g$  of as-cured sample became much lower than  $160^\circ\text{C}$ . Post-curing of these samples gave an improvement of  $\sim 20 \text{ K}$  to their respective  $T_{g,u}$  values. Combined with the observation of varying heating rates, it appears that the heating rate or the residential time as the temperature crosses  $160^\circ\text{C}$  is the most influential factor in determining  $T_{g,u}$ .

Whether the homopolymerization is through  $-\text{OH}$  or  $\text{O}^-$  propagation, both mechanisms yield the same chemical structure of etherification. Thus the difference in the  $T_{g,u}$  may largely be the result of different network structures formed by the various paths. More work is required in the study of gel formation and network development.

In ranking the importance of various factors affecting the  $T_g$ , the order of magnitude of the influence is approximately:

Degree of cure	200 K
Catalyst concentration	$> 50 \text{ K}$
Network structure/curing history	$> 50 \text{ K}$
Purity of monomer	10 K
Physical ageing (reversible)	10 K

The  $T_g$  is increased from the monomeric value of  $-22^\circ\text{C}$  to a probable highest limit of  $\sim 190^\circ\text{C}$  as the degree of cure increases during cure development. However, low  $T_g$ s associated with low degree of cure are subject to increase by further curing.

Although the  $T_g$  depends strongly on EMI concentration, if the concentration is limited to 2–4 phr the influence of EMI concentration alone should be within 10 K. Therefore, even if there is a slight inhomogeneity in the mixture due to mixing procedures, the influence in the present study would be rather minimal.

As shown by this work,  $T_{g,u}$  may be changed by  $> 50 \text{ K}$

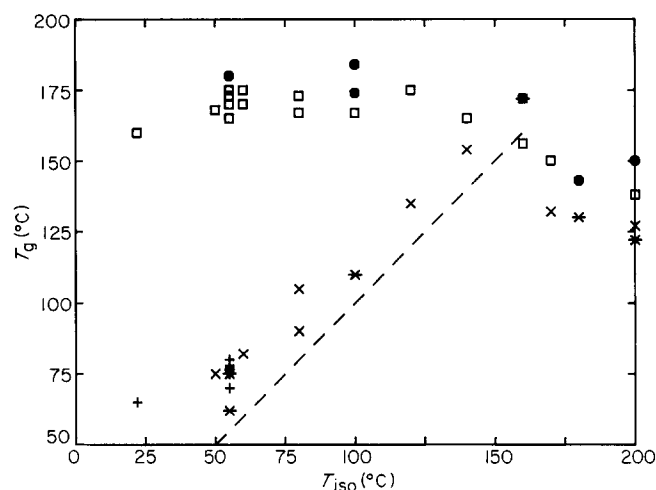


**Figure 11** Glass transition temperature after isothermal cure: (x)  $T_g$  of commercial DGEBA resin with 3 phr EMI after  $T_{iso}$ ; (+)  $T_g$  of commercial DGEBA resin with 3 phr EMI with  $22^\circ\text{C}$  ageing; (□)  $T_{g,u}$  of commercial DGEBA resin with 3 phr EMI after post-cure; (\*)  $T_g$  of recrystallized DGEBA monomer with 3 phr EMI after  $T_{iso}$ ; (●)  $T_{g,u}$  of recrystallized DGEBA monomer with 3 phr EMI after post-cure; (---)  $T_g = T_{iso}$

due to different curing history. It is speculated that even though the heats of cure appeared quite close to each other or the amounts of the functional group reacted remain similar, the network structure and the distribution of different types of crosslinks may be quite different.

As long as the raw material contains  $\leq 10\%$  low molecular weight oligomers, the influence on the final  $T_g$  is in the order of 10 K.

Although the physical ageing, or the thermal history in the vitrification process, may change the state of the glass and hence its  $T_g$  or fictive temperature, the influence is relatively minor and is of the order of 10 K. Furthermore the history of vitrification is erased by heating to temperatures above the  $T_g$ . All cured samples after standing for up to 5 years at room temperature yielded a small hump around 80°C with a peak height of the order of  $0.05 \text{ J g}^{-1} \text{ K}^{-1}$ . This is indicative of an exceptionally wide distribution of a relaxation time spectrum and the glass transition range. Relaxation peaks throughout the glass transition region for crosslinked polymers have been observed by annealing procedures<sup>25</sup>.

Therefore, beyond a region of  $\sim 10 \text{ K}$ , the history of curing is most influential to the attainment of a final  $T_g$  or the  $T_{g,u}$  provided that the chemical composition of the raw resin mixture is kept the same.

## CONCLUSIONS

The  $T_{g,u}$  of the homopolymer of DGEBA epoxy system was observed to vary by  $\sim 70 \text{ K}$  depending on the thermal history of cure, although the extent of reaction as observed from heat release seems to change no more than 10%.

As the oxonium ion  $\text{O}^+$  propagation is considered to be favoured at lower temperatures and the hydroxy group  $-\text{OH}$  propagation at higher temperatures, this gives the impression that the two paths may yield different products. It is not obvious that the two paths of  $\text{O}^+$  or  $-\text{OH}$  propagation should lead to different types of ethereal networks. One may speculate that (1) the potential of the catalyst is not fully developed during the short period of time at fast heating, (2) a loose network is formed in a highly expanded liquid at high temperatures, and (3) the statistics of the encounter of epoxy groups at different temperatures may produce different networks. We believe that the influence of thermal history on network formation should be more universally observable in other systems. In practice, large samples with high activation energy of reaction may show less of the thermal history effect, due to self-accelerating reaction kinetics under a high rate of energy release, as isothermal conditions in these systems cannot be maintained due to low thermal conductivities.

The monitoring of cure development by means of

monitoring the changes in chemical or physical properties or by monitoring the change in the behaviour of guest molecules to an asymptote is commonly applied in industry. In view of the complex polymerization and crosslinking (density and placement) development, these monitoring techniques need to be well calibrated and their range of applicability limited to a narrow window of curing conditions. For *in situ* monitoring, there are not only needs for techniques that are sensitive to the initial viscosity changes for consolidation purposes, but also for techniques that are sensitive to the network structures in the final stages of cure for the determination of the final property.

## REFERENCES

- 1 Farkas, A. and Strohm, P. F. *J. Appl. Polym. Sci.* 1968, **12**, 159
- 2 Dearlove, T. J. *J. Appl. Polym. Sci.* 1970, **14**, 1615
- 3 Barton, J. M. and Sheppard, P. M. *Makromol. Chem.* 1975, **176**, 930
- 4 Ito, M., Hata, H. and Kamagata, K. *J. Appl. Polym. Sci.* 1987, **33**, 1843
- 5 Jisová, V. *J. Appl. Polym. Sci.* 1987, **34**, 2547
- 6 Chang, S. S. *J. Therm. Anal.* 1988, **34**, 135
- 7 Heise, M. S. and Martin, G. C. *J. Polym. Sci., Polym. Lett. Edn* 1988, **26**, 153
- 8 Heise, M. S. and Martin, G. C. *Macromolecules* 1989, **22**, 99
- 9 Heise, M. S. and Martin, G. C. *J. Appl. Polym. Sci.* 1990, **39**, 721
- 10 Heise, M. S., Martin, G. C. and Gotro, J. T. *Polym. Sci. Eng.* 1990, **30**, 83
- 11 Fox, T. G. and Flory, P. J. *J. Appl. Phys.* 1950, **21**, 581
- 12 Chang, S. S. *J. Polym. Sci.* 1984, **C71**, 59
- 13 Ueberreiter, K. and Kanig, C. *J. Chem. Phys.* 1950, **18**, 399
- 14 Fox, T. G. and Loshaek, S. *J. Polym. Sci.* 1955, **15**, 371
- 15 Nielsen, L. E. *J. Macromol. Sci.* 1969, **C3**, 69
- 16 DiMarzio, E. A. *J. Res. Natl Bur. Stand.* 1964, **68A**, 611
- 17 DiBenedetto, A. T. *J. Polym. Sci.* 1987, **B25**, 1949
- 18 Stutz, H., Illers, K.-H. and Mertes, J. *J. Polym. Sci.* 1990, **B28**, 1483
- 19 Hale, A., Macosko, C. W. and Bair, H. E. *Macromolecules* 1991, **24**, 2610
- 20 Plazak, D. J. and Frund Jr, Z. N. *J. Polym. Sci.* 1990, **B28**, 431
- 21 Bauer, R. S. Shell Chem. Co., personal communication, 1986
- 22 Hoehne, G. W. H. and Gloeggler, E. *Thermochim. Acta* 1989, **151**, 295
- 23 Chang, S. S. *Thermochim. Acta* 1991, **178**, 195
- 24 Chang, S. S., Hunston, D. L. and Mopsik, F. I. 'Proc. 4th Ann. Conf. Adv. Composites', ASM International, Materials Park, OH, 1988, p. 91
- 25 Kong, E. S. *Am. Chem. Soc. Ser.* 1983, **211**, 171
- 26 Chang, S. S. *Polym. Commun.* 1988, **29**, 33
- 27 Chang, S. S. in 'Thermal Analysis in Polymer Characterization' (Ed. E. A. Turi), Heyden and Sons, Philadelphia, 1981, p. 89
- 28 Chang, S. S. *Am. Chem. Soc. Polym. Prepr.* 1987, **28**, 244
- 29 Guttman, C. M. personal communication, 1970
- 30 Jones, J. R., Poncipe, C., Barton, J. M. and Wright, W. W. *Polymer* 1987, **28**, 1358
- 31 Ricciardi, F., Joullié, M. M., Romanchick, W. A. and Griscavage, A. A. *J. Polym. Sci., Polym. Lett. Edn* 1982, **20**, 127
- 32 Ricciardi, F., Romanchick, W. A. and Joullié, M. M. *J. Polym. Sci., Polym. Chem. Edn* 1983, **21**, 1475
- 33 Berger, J. and Lohse, F. *J. Appl. Polym. Sci.* 1985, **30**, 531
- 34 Barton, J. M. *Thermochim. Acta* 1983, **71**, 337